EXHIBIT 8

REDACTED

EXHIBIT 9

REDACTED

EXHIBIT 10

REDACTED

EXHIBIT 11

REDACTED

EXHIBIT 12

REDACTED

EXHIBIT 13

REDACTED

EXHIBIT 14

IN THE UNITED STATES DISTRICT COURT
FOR THE DISTRICT OF DELAWARE

AFFYMETRIX, INC., A DELAWARE CORPORATION,	
Plaintiff/Counter-Defendant,	**Civil Action No. 04-901-JJF**
vs.	
ILLUMINA, INC., A DELAWARE CORPORATION,	
Defendant/Counter-Plaintiff.	

DEFENDANT ILLUMINA, INC.'S NOTICE OF SUBPOENA OF DANIEL H. WAGNER ASSOCIATES, INC.

PLEASE TAKE NOTICE that the Subpoena attached hereto as Exhibit 1 was served upon Daniel H. Wagner Associates, Inc., 40 Lloyd Avenue, Suite 200, Malvern, PA 19355-3091.

Dated: January 4, 2006

By:/s/ Richard K. Herrmann
Richard K. Herrmann #405
Mary B. Matterer #2626
MORRIS, JAMES, HITCHENS & WILLIAMS LLP
PNC Bank Center, 10th Floor
222 Delaware Avenue
Wilmington, Delaware 19899-2306
(302) 888-6800
mmatterer@morrisjames.com

11. Prior art" encompasses, by way of example, and without limitation, the subject matter described in each and every subdivision of 35 U.S.C. §§102-103.

12. The requests herein shall be deemed to include any and all relevant documents within your possession, custody or control, including documents located in the personal files of any and all of your past and present managers, agents, representatives, employees, attorneys, consultants and accountants.

13. With respect to any documents withheld on the basis of a claim of attorney-client privilege, attorney work product doctrine, or any applicable claim of privilege or immunity, provide a privilege log describing the documents, including the author(s), the recipient(s), the date and subject matter of the document and the specific ground upon which the refusal to answer is based, including facts supporting the claim of privilege such that Illumina may assess the applicability of the privilege as required by Federal Rule of Civil Procedure 26(b)(5). A description of any attachments or enclosures to the document is also required.

DOCUMENTS AND THINGS TO BE PRODUCED

1. The personnel and/or employment history files for Robert Lipshutz, including without limitation all evaluations, and all employment, partnership, confidentiality and other types of agreements.

2. The personnel and/or employment history files for Luis C. Jevons, including without limitation all evaluations, and all employment, partnership, confidentiality and other types of agreements.

3. The personnel and/or employment history files for Derek H. Bernhart, including without limitation all evaluations, and all employment, partnership, confidentiality and other types of agreements.

4. All documents relating to any payments or consideration paid by Affymax and/or Affymetrix to Wagner Associates.

5. All documents and things relating to U.S. Patent No. 5,795,716 (the '716 Patent) and/or any Related Patents, including the invention and ownership thereof.

6. All communications between you and Affymax and/or Affymetrix concerning or relating to the subject matter described and/or claimed in the '716 Patent and/or any Related Patents.

7. All agreements between Wagner Associates and Affymax and/or Affymetrix.

8. All documents relating to Wagner Associates' policies for seeking and obtaining patents, including policies for assignment of patent rights by employees.

EXHIBIT 15

REDACTED

EXHIBIT 16

REDACTED

EXHIBIT 17

REDACTED

EXHIBIT 18

REDACTED

EXHIBIT 19

REDACTED

EXHIBIT 20

Research Article

Light-Directed, Spatially Addressable Parallel Chemical Synthesis

STEPHEN P. A. FODOR,* J. LEIGHTON READ, MICHAEL C. PIRRUNG,† LUBERT STRYER,‡ AMY TSAI LU, DENNIS SOLAS

Solid-phase chemistry, photolabile protecting groups, and photolithography have been combined to achieve light-directed, spatially addressable parallel chemical synthesis to yield a highly diverse set of chemical products. Binary masking, one of many possible combinatorial synthesis strategies, yields 2^n compounds in n chemical steps. An array of 1024 peptides was synthesized in ten steps, and its interaction with a monoclonal antibody was assayed by epifluorescence microscopy. High-density arrays formed by light-directed synthesis are potentially rich sources of chemical diversity for discovering new ligands that bind to biological receptors and for elucidating principles governing molecular interactions. The generality of this approach is illustrated by the light-directed synthesis of a dinucleotide. Spatially directed synthesis of complex compounds could also be used for microfabrication of devices.

THE REVOLUTION IN MICROELECTRONICS HAS BEEN MADE possible by photolithography, a process in which light is used to spatially direct the simultaneous formation of many electrical circuits. We report a method that uses light to direct the simultaneous synthesis of many different chemical compounds. Synthesis occurs on a solid support. The pattern of exposure to light or other forms of energy through a mask, or by other spatially addressable means, determines which regions of the support are activated for chemical coupling. Activation by light results from the removal of photolabile protecting groups from selected areas (Fig. 1). After deprotection, the first of a set of "building blocks" (for example, amino acids or nucleic acids, each bearing a photolabile protecting group) is exposed to the entire surface, but reaction occurs only with regions that were addressed by light in the preceding step. The substrate is then illuminated through a second mask, which activates a different region for reaction with a second protected building block. The pattern of masks used in these illuminations and the sequence of reactants define the ultimate products and their locations. The number of compounds that can be synthesized by this technique is limited only by the number of synthesis sites that can be addressed with appropriate resolution. Combinatorial masking strategies can be used to form a large number of compounds in a small number of chemical steps. Moreover, a high degree of miniaturization is possible because the density of synthesis sites is bounded only by physical limitations on spatial addressability, in this case the diffraction of light. Each compound is accessible and its position is precisely known. Hence, its interactions with other molecules can be assessed.

Spatially localized photodeprotection. Spatially localized substrate activation can be accomplished by photolithographic techniques. Amino groups at the ends of linkers attached to a glass substrate were derivatized with nitroveratryloxycarbonyl (NVOC), a photoremovable protecting group (*1*). Photodeprotection was effected by illumination of the substrate through a mask (a 100 μm by 100 μm checkerboard) with alternating opaque and transparent elements. The free amino groups were fluorescently labeled by treatment of the entire substrate surface with fluorescein isothiocyanate (FITC). The substrate was then scanned in an epifluorescence microscope. The presence of a high-contrast fluorescent checkerboard pattern with 100 μm by 100 μm elements (depicted in red in Fig. 2) reveals that free amino groups were generated in specific regions by spatially localized photodeprotection.

Light-directed peptide synthesis. Light-directed synthesis of two pentapeptides was carried out as outlined in Fig. 3. The 1-hydroxybenzotriazole (HOBt)–activated ester of NVOC-Leu (NVOC-Leu-OBt) was allowed to react with the entire surface of a substrate that had previously been derivatized with amino functional groups. After removal of the NVOC protecting group by uniform illumination, the substrate was treated with NVOC-Phe-OBt. Two repetitions of this cycle with NVOC-Gly-OBt generated a substrate containing NVOC-GGFL across the entire surface (*2*). Spatially localized photodeprotection was then performed through a 50-μm checkerboard mask. The surface was then treated with *Nα-tert*-butyloxy carbonyl-*O-tert*-butyl-L-tyrosine. Finally, the surface was uniformly illuminated to photolyze the remaining NVOC-GGFL sites and treated with NVOC-Pro-OBt. After removal of the protecting groups, the surface consists of an array of H_2N-Tyr-Gly-Gly-Phe-Leu (YGGFL) and H_2N-Pro-Gly-Gly-Phe-Leu (PGGFL) peptides in 50 μm by 50 μm elements.

Antibody recognition of the peptide pattern. The pentapeptide array was probed with a mouse monoclonal antibody directed against β-endorphin. This antibody (called 3E7) binds YGGFL and YGGFM with nanomolar affinity (*3*) and requires the amino-terminal Tyr for high-affinity binding. A second incubation with fluorescein-labeled goat antibody to mouse was used to detect regions containing bound 3E7. As shown in Fig. 4, a high-contrast (>12:1 intensity ratio) fluorescence checkerboard image shows that

The authors are at the Affymax Research Institute, 3180 Porter Drive, Palo Alto, CA 94304.

*To whom correspondence should be addressed.
†Present address: Department of Chemistry, Duke University, Durham, NC 27706.
‡Present address: Department of Cell Biology, Stanford University School of Medicine, Stanford, CA 94305.

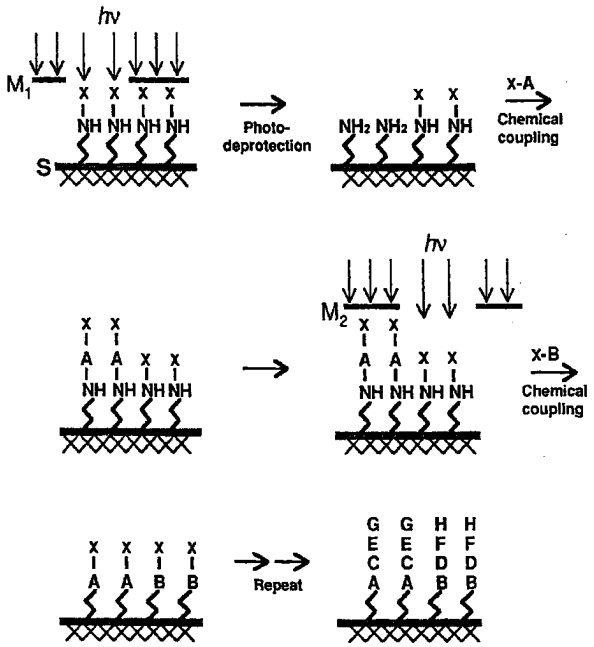

Fig. 1. Concept of light-directed spatially addressable parallel chemical synthesis. A substrate S bears amino groups that are blocked with a photolabile protecting group X. Illumination of specific regions through a lithographic mask M_1 leads to photodeprotection. Amino groups in the exposed sector of the substrate are now accessible for coupling (for example, by the Merrifield solid-phase peptide synthesis method). The first chemical building block A containing a photolabile protecting group X is then attached. A different mask M_2 is used to photoactivate a different region of the substrate. A second labeled group X-B is added and joined to the newly exposed amino groups. Additional cycles of photodeprotection and coupling are carried out to obtain the desired set of products.

(i) YGGFL and PGGFL were synthesized in alternate 50-μm squares, (ii) YGGFL attached to the surface is accessible for binding to antibody 3E7, and (iii) antibody 3E7 does not bind at the PGGFL locations.

A three-dimensional (3-D) representation of the fluorescence intensity data in the checkerboard pattern (Fig. 5) shows that the border between synthesis sites is sharp. The height of each spike in this display is linearly proportional to the integrated fluorescence intensity in a 2.5-μm pixel. The transition between PGGFL and YGGFL occurs within two spikes (5 μm). There is little variation in the fluorescence intensity of different YGGFL squares. The mean intensity of 16 YGGFL synthesis sites was 2.03×10^5 counts, and the standard deviation was 9.6×10^3 counts.

Combinatorial synthesis strategies. In a light-directed chemical synthesis, the products formed depend on the pattern and order of masks and on the order of reactants. For example, consider the four-step synthesis shown in Fig. 6a. The reactants are the ordered set {A,B,C,D}. In the first cycle, illumination through mask m_1 activates the upper half of the synthesis area. Building block A is then added to give the product distribution shown. Illumination through m_2 (which activates the lower half) followed by addition of B yields the next intermediate stage. Building block C is added after illumination through m_3 (which activates the left half), and D is added after illumination through m_4 (which activates the right half) to yield the final product set {AC,AD,BC,BD}.

Extension of the above strategy can then be applied to a large set of building blocks. For example, consider forming the complete set of 400 possible dipeptides from the set of 20 L-amino acids. As shown in Fig. 6b, the synthesis would consist of two synthesis rounds with 20 coupling cycles per round. In cycle 1 of the first round, mask 1 activates 1/20th of the substrate for coupling with the first of 20 amino acids. An additional 19 illumination and coupling cycles are required to complete round 1. The substrate now consists of 20 rectangular stripes each bearing a distinct member of the 20 amino acids. The masks of round 2 are perpendicular to round 1 masks and therefore a single illumination-coupling cycle in round 2 yields 20 dipeptides. The other 19 cycles in round 2 complete the synthesis of the 400 dipeptides. In this combinatorial synthesis strategy, the total number of compounds synthesized (k) would be $k = a^l$, where the length (l) of the peptides is $l = n/a$, n is the number of cycles, and a is the number of chemical building blocks. For example, if $a = 20$ and $l = 5$, then $n = 100$ and $k = 3.2 \times 10^6$.

We develop a general formalism below to describe the combinatorial strategy for any spatially addressable chemical synthesis. The synthesis can be conveniently represented in matrix notation. At each synthesis site, the decision to add a given monomer is inherently a binary process. Therefore, each product element P_j is given by the dot product of two vectors, a chemical reactant vector C = [A,B,C,D] and a binary vector σ_j, which we term a switch vector because it determines whether a reactant appears in a particular product ($P_j = \mathbf{C}\cdot\sigma_j$). Inspection of the products in the first example of Fig. 6 shows that $\sigma_1 = [1,0,1,0]$, $\sigma_2 = [1,0,0,1]$, $\sigma_3 = [0,1,1,0]$, and $\sigma_4 = [0,1,0,1]$. We can now build a switch matrix S from the column vectors σ_j ($j = 1,k$, where k is the number of products).

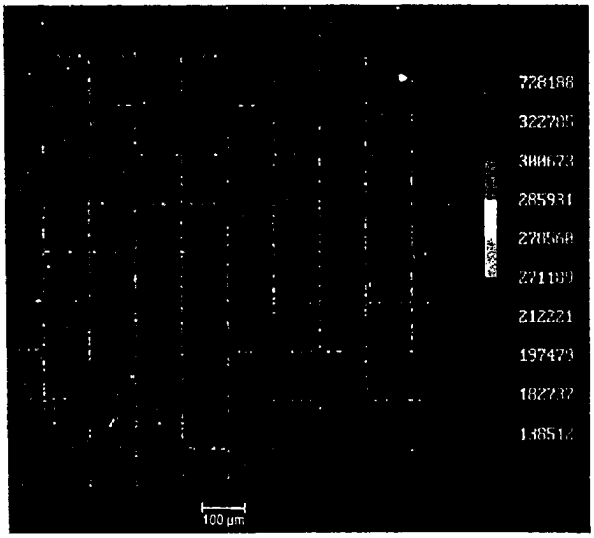

Fig. 2. Spatially localized photodeprotection and fluorescent labeling. Glass microscope slides were cleaned, aminated by treatment with 0.1% aminopropyltriethoxysilane in 95% ethanol, and incubated at 110°C for 20 min. The aminated surface of the slide was then exposed to a 30 mM solution of the *N*-hydroxysuccinimide ester of NVOC-GABA (nitroveratryloxycarbonyl-γ-amino butyric acid) in dimethylformamide (DMF). The NVOC protecting group was photolytically removed by imaging the 365-nm output from a mercury arc lamp through a chrome-on-glass 100-μm checkerboard mask onto the substrate for 20 min at a power density of 12 mW/cm². The exposed surface was then treated with 1 mM FITC in DMF. The substrate surface was scanned with an epifluorescence microscope (Zeiss Axioskop 20, 488-nm excitation from an argon ion laser, Spectra-Physics model 2025). The fluorescence emission above 520 nm was detected by a cooled photomultiplier (Hamamatsu 943-02) operated in a photon-counting mode. Fluorescence intensity was translated into color as shown on the scale on the right (red is the highest intensity).

$$\mathbf{S} = \begin{matrix} \sigma_1 & \sigma_2 & \sigma_3 & \sigma_4 \\ 1 & 1 & 0 & 0 \\ 0 & 0 & 1 & 1 \\ 1 & 0 & 1 & 0 \\ 0 & 1 & 0 & 1 \end{matrix}$$

The outcome **P** of a synthesis is simply **P** = **C S**, the product of the chemical reactant matrix and the switch matrix.

The switch matrix for an n-cycle synthesis yielding k products has n rows and k columns. A key attribute of **S** is that each row specifies a mask. A 2-D mask m_j for the jth chemical step of a synthesis may be obtained directly from the jth row of **S** by placing the elements $s_{j1}, \ldots s_{jk}$ into square format (*4*).

$$\mathbf{S} = \begin{matrix} s_{11} & s_{12} & s_{13} & s_{14} \\ s_{21} & s_{22} & s_{23} & s_{24} \\ s_{31} & s_{32} & s_{33} & s_{34} \\ s_{41} & s_{42} & s_{43} & s_{44} \end{matrix} \qquad m_j = \begin{matrix} s_{j1} & s_{j2} \\ s_{j3} & s_{j4} \end{matrix}$$

For example, the masks in Fig. 6a are then denoted by:

$$m_1 = \begin{matrix} 1 & 1 \\ 0 & 0 \end{matrix} \quad m_2 = \begin{matrix} 0 & 0 \\ 1 & 1 \end{matrix} \quad m_3 = \begin{matrix} 1 & 0 \\ 1 & 0 \end{matrix} \quad m_4 = \begin{matrix} 0 & 1 \\ 0 & 1 \end{matrix}$$

where 1 denotes illumination (activation) and 0 denotes no illumination.

The matrix representation makes it easy to define the masks that generate a desired set of products. Each compound is defined by the product of the chemical vector and a particular switch vector. Therefore, for each synthesis address, a switch vector is chosen, all of the switch vectors are assembled into a switch matrix, and each of the rows is extracted to form the masks. The matrix representation also suggests ways of conducting a synthesis to get particular product distributions or a maximal number of products. For example, for **C** = [A,B,C,D], any switch vector (σ_j) consists of four bits.

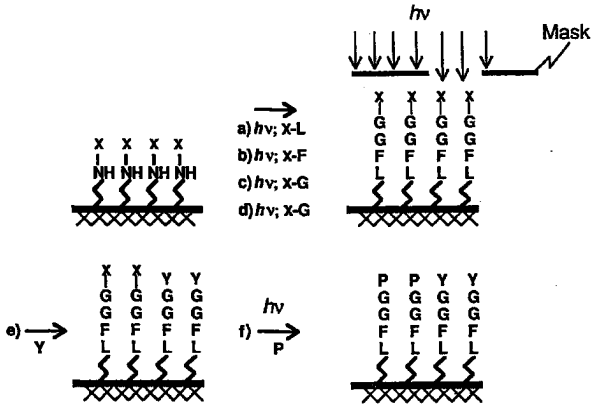

Fig. 3. Experimental scheme for light-directed peptide synthesis. (**a**) Carboxy-activated NVOC-Leu was allowed to react with an illuminated substrate. The carboxy-activated HOBt (1-hydroxybenzotriazole) ester of Leu and other amino acids used in this synthesis was formed by mixing 0.25 mmol of the NVOC amino-protected amino acid with 37 mg HOBt, 111 mg of BOP [benzotriazolyl-*n*-oxy-tris(dimethylamino)-phosphonium hexafluorophosphate], and 86 μl of DIEA (diisopropylethylamine) in 2.5 ml of DMF. (**b**) The NVOC protecting group was removed by uniform illumination as described in Fig. 2, and NVOC-Phe-OBt was coupled to the exposed amino groups for 2 hours at room temperature and then washed with DMF and methylene chloride. (**c** and **d**) Two cycles of photodeprotection and coupling with NVOC-Gly-OBt were carried out. The surface was then illuminated through a 50-μm checkerboard pattern mask. (**e**) Carboxy-activated *Nα-tert*-butyloxy carbonyl-*O-tert*-butyl-L-tyrosine was then added. (**f**) The entire surface was uniformly illuminated to photolyze the remaining NVOC groups. Finally, NVOC-Pro-OBt was added, the NVOC group was removed by illumination, and the *tert*-butyloxy carbonyl and *tert*-butyl protecting groups were removed with trifluoroacetic acid (TFA). These steps lead to a checkerboard pattern of the pentapeptides PGGFL and YGGFL.

Sixteen four-bit vectors exist, [0,0,0,0] to [1,1,1,1]. Hence, a maximum of 16 different products can be made. These 16 column vectors can be assembled in 16! different ways to form a switch matrix. The order of the column vectors defines the masking patterns and therefore the spatial ordering of products, but not their makeup. One readily visualizable ordering of these columns gives a binary switch matrix:

$$\mathbf{S} = \begin{matrix} \sigma_1 & & & & & & & & & & & & & & & \sigma_{16} \\ 1 & 1 & 1 & 1 & 1 & 1 & 1 & 1 & 0 & 0 & 0 & 0 & 0 & 0 & 0 & 0 \\ 1 & 1 & 1 & 1 & 0 & 0 & 0 & 0 & 1 & 1 & 1 & 1 & 0 & 0 & 0 & 0 \\ 1 & 1 & 0 & 0 & 1 & 1 & 0 & 0 & 1 & 1 & 0 & 0 & 1 & 1 & 0 & 0 \\ 1 & 0 & 1 & 0 & 1 & 0 & 1 & 0 & 1 & 0 & 1 & 0 & 1 & 0 & 1 & 0 \end{matrix}$$

Note that the columns of **S** are the binary representations of the numbers 15 to 0. The 16 products of this binary synthesis are ABCD, ABC, ABD, AB, ACD, AC, AD, A, BCD, BC, BD, B, CD, C, D, and Ø (null). Also note that each of the switch vectors from Fig. 6a (and hence the synthesis products) are present in the four-bit binary switch matrix.

The rows of the binary switch matrix have the property that each masking step illuminates one half of the synthesis area. Each masking step also factors the preceding masking step. The half region that was illuminated in the preceding step is again illuminated, whereas the other half is not, and the half region that was unilluminated in the preceding step is also illuminated, whereas the other half is not. Thus masking is recursive. The masks are constructed, as described above, by extracting the elements of each row and placing them in a square array.

$$m_1 = \begin{matrix} 1 & 1 & 1 & 1 \\ 1 & 1 & 1 & 1 \\ 0 & 0 & 0 & 0 \\ 0 & 0 & 0 & 0 \end{matrix} \quad m_2 = \begin{matrix} 1 & 1 & 1 & 1 \\ 0 & 0 & 0 & 0 \\ 1 & 1 & 1 & 1 \\ 0 & 0 & 0 & 0 \end{matrix} \quad m_3 = \begin{matrix} 1 & 1 & 0 & 0 \\ 1 & 1 & 0 & 0 \\ 1 & 1 & 0 & 0 \\ 1 & 1 & 0 & 0 \end{matrix} \quad m_4 = \begin{matrix} 1 & 0 & 1 & 0 \\ 1 & 0 & 1 & 0 \\ 1 & 0 & 1 & 0 \\ 1 & 0 & 1 & 0 \end{matrix}$$

The recursive factoring of masks suggests that the products of a light-directed synthesis can be represented by a polynomial (*5*). For example, the polynomial corresponding to Fig. 6a is

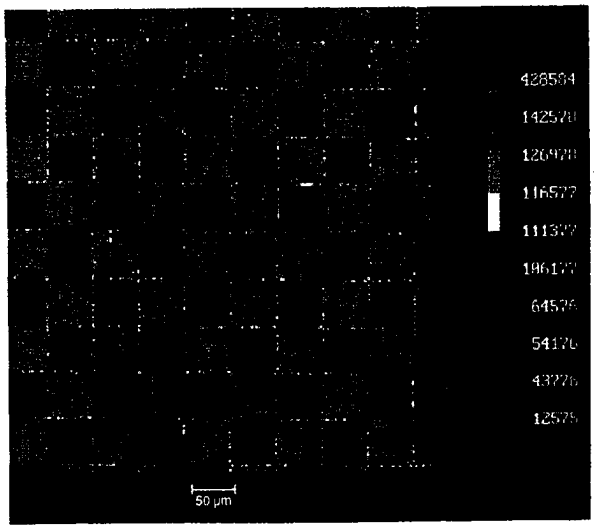

Fig. 4. Fluorescent antibody detection of the YGGFL checkerboard pattern. The array of peptides formed as described in Fig. 3 was incubated with a 2-μg/ml mouse monoclonal antibody (3E7) known to recognize YGGFL (*3*); 3E7 does not bind PGGFL. A second incubation with fluorescein-labeled goat antibody to mouse labeled the regions that bound 3E7. The surface was scanned with an epifluorescence microscope as described in Fig. 2. The fluorescence intensity scale is shown on the right. The alternating bright and dark 50-μm squares show that YGGFL and PGGFL were synthesized in a geometric array determined by the mask depicted in Fig. 3.

$$P = (A + B)(C + D)$$

We can expand a reaction polynomial as though it were an algebraic expression, provided that the order of joining of reactants X_1 and X_2 is preserved, that is, X_1 and X_2 are not commutative ($X_1X_2 \neq X_2X_1$). The product then is AC + AD + BC + BD. The polynomial explicitly specifies the reactants and implicitly specifies the mask for each step. Each pair of parentheses demarcates a round of synthesis. The chemical reactants of a round (for example, A and B) react at nonoverlapping sites and hence cannot combine with one another. The synthesis area is divided equally among the elements of a round (for example, A is directed to one half of the area and B to the other half). Hence, the masks within a round (for example, the masks m_A and m_B) are orthogonal and form an orthonormal set. The polynomial notation also signifies that each element in a round is to be joined to each element of the next round (for example, A with C, A with D, B with C, and B with D). This is accomplished by having m_c overlap m_A and m_B equally, and likewise for m_D. Because C and D are elements of a round, m_c and m_D are orthogonal to each other and form an orthonormal set.

The polynomial representation of the binary synthesis described above, in which 16 products are made from 4 reactants, is

$$P = (A + \varnothing)(B + \varnothing)(C + \varnothing)(D + \varnothing)$$

which gives ABCD, ABC, ABD, AB, ACD, AC, AD, A, BCD, BC, BD, B, CD, C, D, and $\varnothing$ when expanded (with the rule that $\varnothing X = X$ and $X\varnothing = X$, and remembering that joining is ordered). In a binary synthesis, each round contains one reactant and one null (denoted by $\varnothing$). One half of the synthesis area receives the reactant, and the other half receives nothing. Each mask overlaps every other mask to an equal extent (*6*).

Binary syntheses are attractive for two reasons. First, they generate the maximal number of products (2^n) for a given number of chemical steps (n). For four reactants, 16 compounds are formed in the binary synthesis, whereas only 4 are made when each round has two reactants. A 10-step binary synthesis yields 1,024 compounds, and a 20-step binary synthesis yields 1,048,576. Second, products formed in a binary synthesis are a complete nested set with lengths ranging from 0 to n. All of the compounds that can be formed by deleting one or more units from the longest product (with n units) are present. Contained within the binary set are the smaller sets that would be formed from the same reactants with the use of any other set of masks (for example, AC, AD, BC, and BD formed in the synthesis shown in Fig. 6 are present in the set of 16 formed by the binary synthesis). The only potential disadvantage of a binary synthesis is that the experimentally achievable spatial resolution may not suffice to accommodate all of the compounds formed. Therefore, practical limitations may require one to select a particular subset of the possible switch vectors for a given synthesis.

Ten-step binary peptide synthesis. The power of the binary masking strategy can be appreciated by the outcome of a ten-step synthesis that produces 1024 peptides. This synthesis is represented in polynomial notation by (*2,7*)

$$(f + \varnothing)(Y + \varnothing)(G + \varnothing)(A + \varnothing)(G + \varnothing)(T + \varnothing)(F + \varnothing)$$
$$(L + \varnothing)(S + \varnothing)(F + \varnothing)$$

The lengths of the peptides synthesized are given by the binomial distribution. The number of peptides synthesized is 1, 10, 45, 120, 210, 252, 210, 120, 45, 10, and 1 for lengths ranging from 0 to 10 amino acids, respectively (the mean is 5).

A fluorescence scan of the resulting peptide array after antibody staining is shown in Fig. 7a. The 32 by 32 peptide array (1024 peptides) is clearly evident. Each synthesis site is a 400-μm by 400-μm square. The identity of the peptide in each square can be ascertained by examining the coordinate map shown in Fig. 7b. The scan shows a range of fluorescence intensities, from a background value of 3,300 counts to 22,400 counts in the brightest square (x = 20 and y = 9). Only 15 compounds exhibit an intensity greater than 12,300 counts. The median value of the array is 4800 counts.

It would be desirable to deduce a binding affinity of a given peptide from the measured fluorescence intensity. Conceptually, the

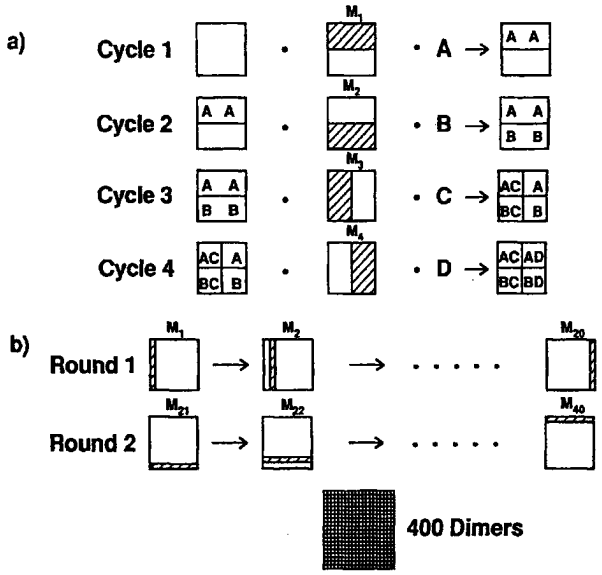

Fig. 6. (**a**) Masks used to synthesize AC, AD, BC, and BD from reactants A, B, C, and D. The synthesis consists of four photolysis and chemical coupling cycles. (**b**) Extension of the above masking strategy for the synthesis of all 400 dipeptides from the 20 naturally occurring amino acids. The synthesis consists of two rounds, with 20 photolysis and chemical coupling cycles per round. In the first cycle of round 1, mask 1 activates 1/20th of the substrate for coupling with the first of 20 amino acids. Nineteen subsequent illumination-coupling cycles in round 1 yield a substrate consisting of 20 rectangular stripes each bearing a distinct member of the 20 amino acids. The masks of round 2 are perpendicular to round 1 masks, and therefore a single illumination-coupling cycle in round 2 yields 20 dipeptides. Twenty illumination-coupling cycles of round 2 complete the synthesis of the 400 dipeptides.

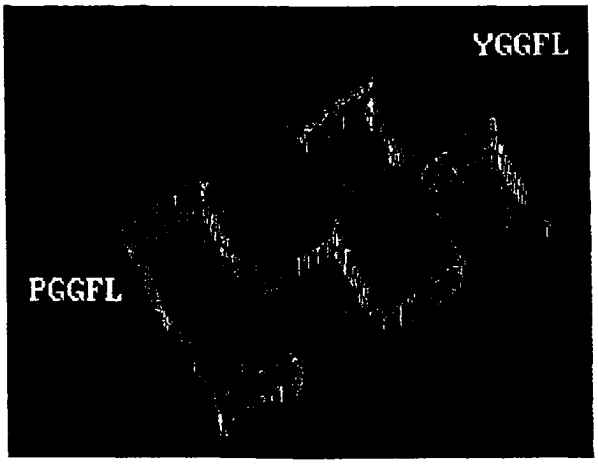

Fig. 5. Three-dimensional representation of the checkerboard array of YGGFL and PGGFL. Fluorescence intensity data shown by color in Fig. 4 were converted into spike heights that are proportional to the number of counts detected from 2.5-μm square pixels. The spikes are also color coded.

simplest case is one in which an univalent receptor binds to a single peptide. The fluorescence scan is carried out after the slide is washed with buffer for a defined time. The order of fluorescence intensities is then primarily a measure of the relative dissociation rates of the antibody-peptide complexes. If the on-rate constants are the same (for example, if they are diffusion-controlled), the order of fluorescence intensities corresponds to the order of binding affinities. However, the situation here is more complex because a bivalent primary antibody and a bivalent secondary antibody were used. The density of peptides in a synthesis area corresponded to a mean separation of ~7 nm, which would allow multivalent antibody-peptide interactions. Hence, the fluorescence intensities depicted in Fig. 7a should be regarded as qualitative indicators of binding affinity (*8*).

Another important consideration is the fidelity of synthesis. Deletions are produced by incomplete photodeprotection or incomplete coupling. The net coupling yield per cycle in these experiments is typically between 85 and 95 percent (*9*). Implementing the switch matrix by masking is imperfect because of light diffraction, internal reflection, and scattering. Consequently, "stowaways" (chemical units that should not be incorporated) arise by unintended illumination of regions that should be dark. A binary synthesis array contains many of the internal controls needed to assess the fidelity of a synthesis. For example, the fluorescence signal from a synthesis area nominally containing a tetrapeptide ABCD could come from a tripeptide deletion impurity such as ACD. Such an artifact would be ruled out by the finding that the fluorescence intensity of the ACD site is less than that of the ABCD site.

The fifteen most highly labeled peptides in the array shown in Fig. 7a are YGAFLS, YGAFS, YGAFL, YGGFLS, YGAF, YGALS, YGGFS, YGAL, YGAFLF, YGAF, YGAFF, YGGLS, YGGFL, YGAFSF, and YGAFLSF. A striking feature is that all 15 begin with YG, which agrees with previous work (*3*) showing that an amino-terminal Tyr is a key determinant of binding. Residue 3 of this set is either A or G, and residue 4 is either F or L; S and T are excluded from these positions. Our finding that the preferred sequence is YG (A/G) (F/L) is in accord with a recent study in which a large library of peptides on phage generated by recombinant DNA methods was screened for binding to antibody 3E7 (*10*). Additional binary syntheses based on leads from peptides on phage experiments show that YGAFMQ, YGAFM, and YGAFQ give stronger fluorescence signals than does YGGFM, which is more closely related to the immunogen used to obtain 3E7 (*3*).

Oligonucleotide synthesis. The generality of light-directed spatially addressable parallel chemical synthesis is demonstrated by its application to nucleic acid synthesis. Light-activated formation of a thymidine-deoxycytidine dinucleotide was carried out as described in Fig. 8. 5′-Nitroveratryl thymidine was attached to the surface of a glass substrate. After removal of the protecting group by illumination through a 500-μm checkerboard mask, the substrate was treated with a phosphoramidite-activated derivative of deoxycytidine. A fluorescent probe was then attached to the exocyclic NH_2

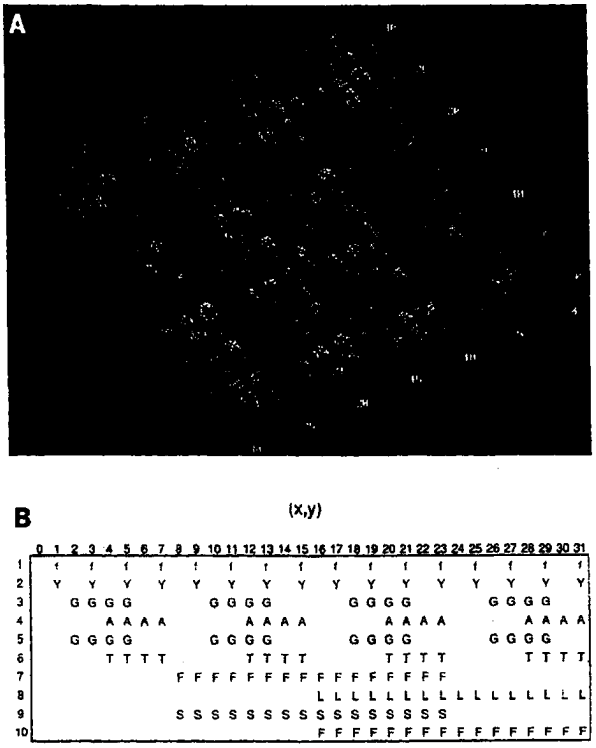

Fig. 7. (**a**) Fluorescence scan of an array of 1024 peptides generated by a ten-step binary synthesis. Following photochemical and side group deprotection, the array was treated with antibody 3E7 and then fluorescein-labeled antibody as described in the preceding legends. The polynomial expression for this ten-step binary synthesis is

$$(J + \varnothing)(Y + \varnothing)(G + \varnothing)(A + \varnothing)(G + \varnothing)(T + \varnothing)(F + \varnothing)(L + \varnothing)(S + \varnothing)(F + \varnothing)$$

Each peptide occupies a 400 μm by 400 μm square. (**b**) Coordinate map for the ten-step binary synthesis. The identity of each peptide in the array can be determined from its x and y coordinates (each range from 0 to 31). The chemical units at sequence positions 1, 3, 4, 7, and 8 are specified by the x coordinate (blue) and those at positions 2, 5, 6, 9, and 10 by the y coordinate (red). All but one of the peptides is shorter than ten residues. For example, to identify the peptide at $x = 12$ and $y = 3$, extract the blue members from column 12 (. .GA..F . . .) and the red members from column 3 (.Y. .G. . . . .) while preserving the linear order to obtain the sequence YGAGF. The brightest element of the array, YGAFLS, is at $x = 20$ and $y = 9$.

Fig. 8. Three-dimensional representation of a fluorescence scan showing a checkerboard pattern generated by the light-directed synthesis of a dinucleotide. 5′-Nitroveratryl thymidine was synthesized by published procedures (*22*) from the 3′-*O*-thymidine acetate. After deprotection with base, the 5′-nitroveratryl thymidine was attached to an aminated substrate through a linkage to the 3′-hydroxyl group. The nitroveratryl protecting groups were removed by illumination through a 500-μm checkerboard mask. The substrate was then treated with phosphoramidite-activated 2′-deoxycytidine. In order to follow the reaction fluorometrically, the deoxycytidine had been modified with an FMOC-protected aminohexyl linker attached to the exocyclic amine {5′-*O*-(4,4′-dimethoxytrityl)-4-*N*-[6-*N*-fluorenylmethylcarbamoylhexylcarboxy (FMOC)]-2′-deoxycytidine} (*23*). After removal of the FMOC protecting group with base, the regions which contained the dinucleotide were fluorescently labeled by treatment of the substrate with 1 mM FITC in DMF for 1 hour.

group of deoxycytidine (see Fig. 8).

The 3-D representation of the fluorescence intensity data in Fig. 8 reproduces the checkerboard illumination pattern used during photolysis of the substrate. This result demonstrates that oligonucleotides as well as peptides can be synthesized by the light-directed method.

Comparison to other methods and potential applications. We have introduced an approach for the simultaneous synthesis of a large number of compounds that combines solid-phase synthesis (*11*), photolabile protecting groups (*1*), and photolithography (*12*). The method can be applied to any solid-phase synthesis technique in which light can be used to generate a reactive group. We have used light-directed spatially addressable parallel chemical synthesis to synthesize large arrays of peptides. The light-directed formation of oligonucleotides attests to the versatility of the technique and suggests that it could be broadly applicable in making high-density arrays of chemical compounds. The ten-step binary synthesis results in the formation of 1024 peptides in 1.6 cm^2. The 50-μm checkerboard pattern of alternating pentapeptides shows that 40,000 compounds can be synthesized in 1 cm^2. Our present capability for high-contrast photodeprotection is better than 20 μm, which gives >250,000 synthesis sites per square centimeter. There is no physical reason why higher densities of synthesis sites cannot be achieved. Indeed, high spatial resolution electron-beam lithography (~250 Å) has been used to generate patterns at a density of 10^{10} per square centimeter (*13*).

It is interesting to compare the light-directed method with other techniques for parallel chemical synthesis. One approach is to physically segregate different reactants by pipeting them into different reaction vessels. For example, 96 peptides have been simultaneously synthesized on the tips of pins by immersing them into different solutions that are contained in the chambers of a microtiter plate (*14*). The need for physical separation of reaction sites sharply limits the number of compounds that can be made by the pin method. In contrast, very large numbers of peptides can be generated by recombinant DNA approaches (*9, 15*). Millions of different peptide sequences can be expressed on the surface of phage by inserting randomly synthesized oligonucleotides into their genomes. Each phage clone displays a different peptide. Although the peptides-on-phage are in suspension and are not fixed at defined locations, those that bind tightly to a receptor can be identified by panning, isolation of individual clones, and DNA sequencing. Only peptides that contain genetically coded amino acids can be generated by expression on phage. The recombinant and light-directed approaches have distinctive strengths that are complementary. For example, a peptide identified by the phage method to have appreciable affinity for a receptor can serve as the kernel around which diversity is generated by light-directed synthesis. A synthesis might include custom chemical building blocks in addition to the standard set of L-amino acids (*16*). For example, D-amino acids could be introduced to make the peptide more resistant to proteolysis (*17*), and modified site chains (*18*) could be inserted to increase affinity.

Parallel chemical synthesis could be used to explore molecular recognition processes in biology and other fields. For example, pharmaceutical discovery is increasingly based on an understanding of the way receptors and enzymes interact with specific ligands. The techniques described here allow the synthesis of large numbers of peptides or other oligomers that can be surveyed for binding to biological macromolecules.

Fabrication of small devices such as microelectronic circuits relies on the chemistry of photoresists, vapor deposition, and ion implantation. The techniques described here enable the in situ synthesis of complex compounds on a microscale. The methods of spatially addressable chemical synthesis may be used in conjunction with the microfabrication of circuitry. The union of these technologies may find applications in novel detection devices containing arrays of biological receptors or other molecular recognition elements.

The functional properties of molecules synthesized by the light-directed approach can be read in a variety of ways. As was shown here, the binding of a receptor such as an antibody can readily be detected fluorimetrically. Radioactive or chemiluminescent labels could also be used (*19*). The susceptibility of compounds in an array to modification by an enzyme or other catalyst could also be directly assayed. For example, the cleavage of a peptide at a site located between a fluorescent energy donor and acceptor would lead to increased fluorescence (*20*). Peptides that are effective substrates for phosphorylation by a kinase could be identified by monitoring the ^{32}P pattern following incubation with enzyme and radiolabeled ATP (adenosine triphosphate).

Oligonucleotide arrays produced by light-directed synthesis could be used to detect complementary sequences in DNA and RNA. Such arrays would be valuable in gene mapping, fingerprinting, diagnostics, and nucleic acid sequencing. A sequencing method based on hybridization to a complete set of fixed-length oligonucleotides immobilized individually as dots of a two-dimensional matrix has been proposed (*21*). It is noteworthy that the light-directed synthesis of all 65,536 possible octanucleotides (4^8) would fit into 1.6 cm^2 with 50-μm square sites, a resolution already achieved.

REFERENCES AND NOTES

1. A. Patchornik, B. Amit, R. B. Woodward, *J. Am. Chem. Soc.* **92**, 6333 (1970). There is a wide array of available photochemical protecting groups [V. N. R. Pillai, *Synthesis* **1980**, 1 (1980)]. We have used NVOC because of its favorable absorption characteristics and its established use in peptide synthesis.
2. One-letter codes for the amino acids (L-isomers except for G, Gly): A, Ala; F, Phe; L, Leu; M, Met; P, Pro; Q, Gln; S, Ser; T, Thr; and Y, Tyr. Lower-case one-letter codes are reserved for the D-isomers.
3. T. Meo *et al.*, *Proc. Natl. Acad. Sci. U.S.A.* **80**, 4084 (1983).
4. Compounds formed in a light-activated synthesis can be positioned in any defined geometric array as long as equivalent transformations are used for each row. A square or rectangular matrix is convenient but not required.
5. Not all light-activated syntheses can be represented as factored polynomials. Some can only be denoted by irreducible (prime) polynomials.
6. Binary rounds and nonbinary rounds can be interspersed as desired, as in

$$P = (A + \emptyset)(B)(C + D + \emptyset)(E + F + G)$$

The 18 compounds formed are ABCE, ABCF, ABCG, ABDE, ABDF, ABDG, ABE, ABF, ABG, BCE, BCF, BCG, BDE, BDF, BDG, BE, BF, and BG. The switch matrix S for this seven-step synthesis is

$$S = \begin{matrix} 1111111110000000000 \\ 1111111111111111111 \\ 1111000000111000000 \\ 0001110000000111000 \\ 1001001001001001001 \\ 0100100100100100100 \\ 0010010010010010010 \end{matrix}$$

The round denoted by (B) places B in all products because the reaction area was uniformly activated (the mask for B consisted entirely of 1's). The number of compounds k formed in a synthesis consisting of r rounds, in which the ith round has b_i chemical reactants and z_i nulls, is

$$k = \Pi\,(b_i + z_i),$$

and the number of chemical steps n is

$$n = \Sigma\, b_i.$$

The number of compounds synthesized when $b = a$ and $z = 0$ in all rounds is a^n/a, compared with 2^n for a binary synthesis. For $n = 20$ and $a = 5$, 625 compounds (all tetramers) would be formed, compared with 1.049×10^6 compounds in a binary synthesis with the same number of chemical steps. It should also be noted that rounds in a polynomial can be nested, as in

$$[(A + (B + \emptyset)(C + \emptyset)]\,(D + \emptyset)$$

The products are AD, BCD, BD, CD, D, A, BC, B, C, and Ø.

7. The longest peptide formed is fYGAGTFLSF (the amino-terminal is f and the carboxyl-terminal residue linked to the substrate is F). Because the solid-phase synthesis is carried out in the carboxyl-to-amino direction, F is the first, S is the second, and f is the tenth unit to be coupled.
8. In cases where the monovalent interaction of a receptor with a ligand is very low (where the off rate is rapid), it may not be possible to detect the binding of the

receptor to the surface-immobilized compounds. In such cases, multivalency can be used to decrease the off rate by forming multimers of the receptor with cross-linking reagents or by preincubating the receptor with a nonblocking immunoglobulin G (IgG).

9. The contribution to the net coupling yield from photodeprotection and chemical coupling has been assessed in the following ways. We have experimentally determined the photolysis rate for NVOC–amino acids and have chosen illumination conditions that ensure >99 percent of the amino acids have been photodeprotected. We have also determined the chemical coupling efficiency of selected amino acids on our substrates. For example, in order to determine the coupling efficiency of Leu to Leu, NVOC was first selectively photolyzed from one region of a NVOC–Leu derivatized substrate. The photochemically deprotected amino groups in this first region were then coupled to FMOC-Leu-OBt. At this stage incomplete Leu to Leu coupling would leave unreacted amino groups. A second photolysis step was then used to photolyze a different region of the substrate. Treatment of the substrate with FITC would label the free amino groups that remain from incomplete chemical coupling in the first region and the free amino groups exposed by photolysis in the second region. Direct comparison of the quantitative fluorescence signal from both regions indicates the extent of chemical coupling. If the coupling yield is high, the ratio of the signals of the first to the second photolysis regions is low. We have used this technique as an optimization tool in order to develop the experimental conditions that maximize chemical coupling.
10. S. E. Cwirla, E. A. Peters, R. W. Barrett, W. J. Dower, *Proc. Natl. Acad. Sci. U.S.A.* **87**, 6378 (1990).
11. B. Merrifield, *Science* **232**, 341 (1986).
12. D. A. McGillis, in *VLSI Technology*, S. M. Sze, Ed. (McGraw-Hill, New York, 1983), pp. 267–301.
13. T. H. Newman, K. E. Williams, R. F. W. Pease, *J. Vac. Sci. Technol. B* **5**, 88 (1987).
14. H. M. Geysen, S. J. Rodda, T. J. Mason, *Ciba Found. Symp.* **119**, 131 (1986); ———, G. Tribbick, P. G. Schoofs, *J. Immunol. Methods* **102**, 259 (1987).
15. J. K. Scott and G. P. Smith, *Science* **249**, 386 (1990); J. J. Devlin, L. C. Panganiban, P. E. Devlin, *ibid.*, p. 404. For selection of tightly bound randomly generated RNA sequences, see C. Tuerk and L. Gold, *ibid.*, p. 505 (1990); A. D. Ellington and J. W. Szostak, *Nature* **346**, 818 (1990).
16. Suppose that the kernel consists of PQR separated from XYZ and that the aim is to synthesize peptides in which these units are separated by a variable number of different residues. The kernel can be placed in each peptide by using a mask that has 1's everywhere. The polynomial representation of a suitable synthesis is

$$(P)(Q)(R)(A + \varnothing)(B + \varnothing)(C + \varnothing)(D + \varnothing)(X)(Y)(Z)$$

Sixteen peptides would be formed, ranging in length from the six-residue PQRXYZ to the ten-residue PQRABCDXYZ. Other masking strategies deserve comment. For example, by using a particular mask more than once, we compel two or more reactants to appear in the same set of products. Suppose that the mask for an eight-step synthesis is

A	11110000
B	00001111
C	11001100
D	00110011
E	10101010
F	01010101
G	11110000
H	00001111

The products are ACEG, ACFG, ADEG, ADFG, BCEH, BCFH, BDEH, and BDFH. A and G always appear together because their additions were directed by the same mask, and likewise for B and H.
17. J. J. Nestor, Jr., R. Tahilramani, T. L. Ho, G. I. McRae, B. H. Vickery, *J. Med. Chem.* **31**, 65 (1988).
18. M. H. Gelb, J. P. Svaren, R. H. Abeles, *Biochemistry* **24**, 1813 (1985).
19. We have used fluorescence because it is a convenient, rapid, and highly sensitive mode of detection. Our detection system has a sensitivity limit of ~100 fluorescein molecules in a 10-μm^2 region. We have not explored the limits of detection for other physical techniques.
20. S. A. Latt, D. S. Auld, B. L. Vallee, *Anal. Biochem.* **50**, 56 (1972); E. D. Matayoshi, G. T. Wang, G. A. Krafft, J. W. Erickson, *Science* **247**, 954 (1990).
21. K. R. Khrapko *et al.*, *FEBS Lett.* **256**, 118 (1989).
22. E. Ohtsuka, S. Tanaka, M. Ikehara, *Synthesis* **1977**, 453 (1977).
23. A. Roget, H. Bazin, R. Teoule, *Nucleic Acids Res.* **17**, 7643 (1989).
24. We are grateful to R. F. W. Pease for his advice on photolithography and R. A. Mathies for helpful suggestions on fluorescence microscopy. We also thank R. Hale, J. Winkler, P. Yu-Yang, and S. M. Gruber for their excellent technical assistance.

23 October 1990; accepted 15 January 1991